PCCP

Accepted Manuscript

ROYAL SOCIETY OF CHEMISTRY

www.rsc.org/pccp

ARTICLE Journal Name

The cooperative adsorption properties of cetyl/amino-SBA-15 for 4-nonylphenol

Received 00th January 20xx,
Accepted 00th January 20xx

DOI: 10.1039/x0xx00000x

www.rsc.org/

Feng Quan, Yun Hu*, Xingchen Liu, Chaohai Wei

In this study, cetyl and amino groups bifunctionalized mesoporous SBA-15 (cetyl/amino-SBA-15) was prepared successfully by a post-synthesis grafting method. Detailed characterization by XRD, FT-IR, N_2 adsorption-desorption and elemental analysis confirmed that the cetyl/amino-SBA-15 still retained the long-range ordered hexagonal mesostructure. Cetyl and aminopropyl groups were simultaneously functionalized on the surface of SBA-15. The adsorption capacity of cetyl/amino-SBA-15 was much higher than that of the arithmetic summation of cetyl-SBA-15 and amino-SBA-15, due to the cooperative effect of the hydrogen bond/electrostatic interaction between 4-nonylphenol (4-NP) and aminopropyl groups and hydrophobic interactions between 4-NP and cetyl groups. The effects of dosage and mole ratio of cetyl and amino groups on the adsorption properties of cetyl/amino-SBA-15 for 4-NP were also investigated. Cetyl/amino-SBA-15 exhibited excellent adsorption capacity over a wide range of pH values, and cetyl/amino-SBA-15(3.2/0.8) showed the highest adsorption capacity up to 120 mg/g. Furthermore, cetyl/amino-SBA-15 exhibited high adsorption selectivity for 4-NP against phenol as well as high reusability, showing a great potential for wastewater treatment applications.

1. Introduction

4-Nonylphenol (4-NP) is an important chemical raw material and intermediate, widely used in the production of nonylphenol ethoxylate surfactants, pesticide emulsifiers, antioxidants, and lubricatingoil additives.[1] The global production of 4-NP increased to 314,340 tonnes per year in 2011.[2] An endocrine disruptor, 4-NP may cause disruption of the hormone system and the reproductive system by mimicking the structure of the natural hormone. The compound 4-NP has been detected in food,[3,4] air,[5] ground water,[6,7] soil[8,9] and oceans.[10] The main methods of removing 4-NP include biological treatment,[11-13] advanced oxidation technology[14-16] and adsorption methods.[17-19] The adsorption method is considered a simple and efficient method,[20,21] because it could effectively separate 4-NP from aqueous solutions at low concentrations and reduce the environmental risks of 4-NP.

Ordered mesoporous materials were prepared by the self-assembly of surfactants, have attracted wide attention in many fields including adsorbent, catalyst, drug delivery agent and sensor, due to the high specific surface area, highly uniform pore size distribution and large pore volume. [22-26] These materials exhibit various morphologies under various synthetic conditions, such as nanoparticle, monolith and film morphologies.[27-29] Ordered mesoporous silica is widely used as adsorbent due to a large number of easy functionalized silanol groups on the surface. However, unmodified ordered mesoporous silica has low hydrothermal stability, low adsorption capacity and poor selectivity due to the strong hydrophilicity. Many researchers have focused on the organic surface modification of ordered mesoporous silica to enhance its adsorption capacity or selectivity for organic pollutants. Inumaru et al.[30] reported that octyl-grafted MCM-41 showed a high selectivity for 4-NP from aqueous solutions. Kim et al.[31] found that phenyl-functionalized MCM-41 showed a high adsorption capacity for *p*-*t*-butylaniline due to the interactions of the phenyl groups and Si-OH. The adsorption capacities of adsorbents are closely related to the adsorption interactions between adsorbents and target pollutants. Previous research has focused mainly on the preparation of single functional group grafted adsorbents. However, the selectivity of the monofunctionalized adsorbents for target pollutants is limited in low concentration aqueous solutions. To achieve more satisfactory adsorption performance including adsorption capacity and selectivity, the multifunctionalized adsorbents are introduced into the adsorption field.[32-35] The organic functional groups on the surface of multifunctionalized adsorbents could selectively bind certain functional groups of target pollutants by different adsorption interactions, resulting in stronger adsorption interactions and higher adsorption capacity. Zhang et al.[36] prepared diamine/phenyl-SBA-15, which could effectively remove eosin at low concentrations from wastewater and exhibited high selectivity for eosin.

According to the molecular characteristics of 4-NP, namely, 4-NP contains both nonyl and phenolic hydroxyl groups, hexadecyltrimethoxysilane and aminopropyltrimethoxysilane were chosen for the modification of SBA-15. Cetyl/amino-SBA-15 was prepared successfully by a post-synthesis grafting method. Compared with monofunctionalized SBA-15, the cooperative effect between cetyl and aminopropyl groups significantly improved the adsorption capacity of SBA-15 for 4-NP. To investigate the cooperative effect mechanism and the roles of aminopropyl and cetyl groups on adsorption of 4-NP further, the exploration on the effect of different cetyl/amino mole ratios was carried out. Moreover, amino-, diamino- and triamino-silanes were chosen to investigate the effect of -NH/-NH_2 sites on the adsorption of 4-NP. In addition, the selective adsorption and regeneration performance of cetyl/amino-SBA-15 were investigated.

The Key Lab of Pollution Control and Ecosystem Restoration in Industry Clusters, Ministry of Education, School of Environment and Energy, South China University of Technology, Guangzhou 510006, P. R. China
E-mail address: huyun@scut.edu.cn (Y. Hu)
Tel: +86-20-39380573
Fax: +86-20-39380588

2. Experimental Section

2.1. Materials

Pluronic P123 (Mw=5800, $EO_{20}PO_{70}EO_{20}$, Sigma-Aldrich), tetraethoxysilane (TEOS, Tianjin Fuchen Chemical Reagents Factory) and hydrochloric acid (HCl, Guangzhou Chemical Reagent Factory) were used for the synthesis of SBA-15. Hexadecyltrimethoxysilane (cetylsilane), 3-aminopropyltrimethoxy-silane (aminosilane), N-[3-trimethoxysilylpropyl]ethylenediamine (diaminosilane) and N-[3-trimethoxysiylpropyl]diethylenetriamine (triaminosilane) were purchased from Sigma-Aldrich for the modification of SBA-15. 4-Nonylphenol (4-NP) and phenol (Ph) were supplied by Aladdin. All chemicals were used as received without further purification.

2.2. Synthesis of SBA-15

The SBA-15 sample was prepared as described previously.[37] In a typical preparation procedure, 2.0 g of P123 was dissolved in 15 mL of distilled water and 60 mL of HCl (2 M) and stirred 2 h to obtain a transparent solution under 40 °C. 4.6 mL of TEOS was added dropwise to the above solution with vigorous stirring, and the stirring was maintained for 20 h. The resulting gel was then aged for 24 h at 100 °C. The product was obtained by filtration, washed with distilled water and dried at 100 °C. After calcining at 550 °C for 6 h, the SBA-15 sample was obtained.

2.3. Synthesis of functionalized SBA-15

The bifunctionalized SBA-15 was obtained by a post-synthesis grafting method. Typically, 0.5 g of dried SBA-15 was suspended in 50 mL of dry toluene containing a certain amount of cetylsilane and aminosilane (diamino- or triaminosilane), which was refluxed at 110 °C for 12 h. The sample was obtained by filtration, washed with isopropyl alcohol and dried at 100 °C. The bifunctionalized SBA-15 was denoted as cetyl/amino-SBA-15(x/y) (cetyl/diamino-SBA-15 or cetyl/triamino-SBA-15), where x and y were the mole number of cetylsilane and aminosilane (diamino- or triaminosilane), respectively. The monofunctionalized adsorbents, amino-SBA-15 and cetyl-SBA-15, were prepared with the same method by using only aminosilane or cetylsilane as the silane modifier. The physical mixture sample was prepared by grinding method using same mass of cetyl-SBA-15 and amino-SBA-15.

2.4. Characterization

Powder X-ray diffraction (XRD) patterns of prepared samples were obtained using a Bruker D8 Advance diffractometer (Cu Kα, λ=0.15418 nm), operated at 40 kV and 40 mA between 0.6° and 5° (2θ) with a step length of 0.02° and a scanning rate of 0.4 s per step. CHN elemental analysis was performed using an Elementar Vario EL Cube elemental analyzer. Nitrogen adsorption-desorption isotherms were conducted at 77 K with a Micromeritics ASAP2020 specific surface area analyzer. Fourier transform infrared (FT-IR) spectra were measured on a Thermo Nicolet-6700 in the range of 4000-400 cm^{-1} with KBr disks containing the prepared samples.

2.5. Isothermal adsorption experiment and analysis methods

The prepared samples (10 mg) were mixed with 3.0 mg/L of 4-NP aqueous solutions, the volume of NP aqueous solutions ranging from 100 to 800 mL. Next, the mixed solutions were placed in a temperature-controlled water bath shaker with a shaking speed of 170 rpm for 4 h at 25 °C. The particles were filtered by a 0.45 μm membrane filter with a disposable syringe. The residual concentration of 4-NP was measured by a high performance liquid chromatography (HPLC). HPLC was performed on a Shimadzu LC-20A with an AMP C18 chromatographic column and detected at 275 nm. Methanol/water (90/10, v/v) was used as the mobile phase at 1.000 mL/min.

The equilibrium adsorption amount (Qe mg/g) of 4-NP was calculated as eq. 1:

$$Qe=\frac{V(C_0-C_e)}{m} \quad (1)$$

where C_0 and C_e are the initial and equilibrium concentration (mg/L), V is the volume of the solution (L), and m is the mass of the prepared samples (g).

2.6. Selective adsorption experiment

Selective adsorption experiments were carried out in mixed 4-NP and Ph solutions using cetyl/amino-SBA-15(3.2/0.8) as an adsorbent. 10 mg of the prepared samples were placed in 200 mL of mixed solutions with different concentrations (mmol/L), $C_{4\text{-}NP}$:C_{Ph} ranging from 1:1 to 1:60.

The selective adsorption coefficient ($K_{4\text{-}NP,Ph}$) was calculated by eq. 2 and eq. 3:[38,39]

$$K_{4-NP}=\frac{M^a_{4-NP}}{M^s_{4-NP}} \quad (2)$$

$$K_{4-NP,Ph}=\frac{K_{4-NP}}{K_{Ph}} \quad (3)$$

where $K_{4\text{-}NP}$ and K_{Ph} represent for the adsorption distribution coefficients of 4-NP and Ph, and M^s_{4-NP} and M^a_{4-NP} stand for the mole fractions of 4-NP in solution and adsorbed in the adsorbent.

3. Results and discussion

3.1. Structural analyses of SBA-15 and functionalized SBA-15

Fig. 1 shows the small-angle XRD patterns of SBA-15 and functionalized SBA-15 samples. In accordance with previous reports, a high intensity diffraction peak at approximately 1° was assigned to (100) reflection planes, and two clear broad peaks in the range of 1.5-2° were assigned to (110) and (200) reflection planes,[40] indicating that the prepared samples have a typical long-range ordered hexagonal mesostructure. As seen in Fig. 1 (b), with the increase in addition dose of organic modifier, the (100), (110)

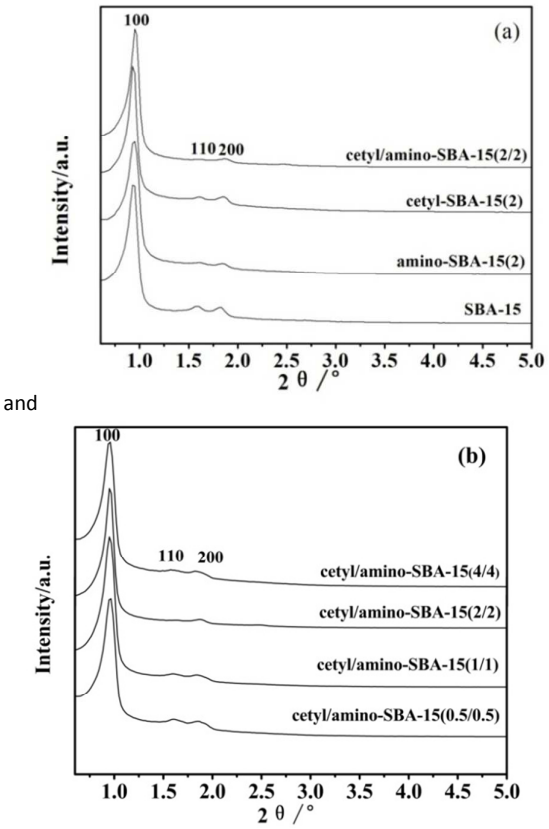

Fig. 1. XRD patterns of SBA-15 and functionalized SBA-15: (a) SBA-15, cetyl-SBA-15(2), amino-SBA-15(2) and cetyl/amino-SBA-15(2/2); (b) cetyl/amino-SBA-15 with different dosage.

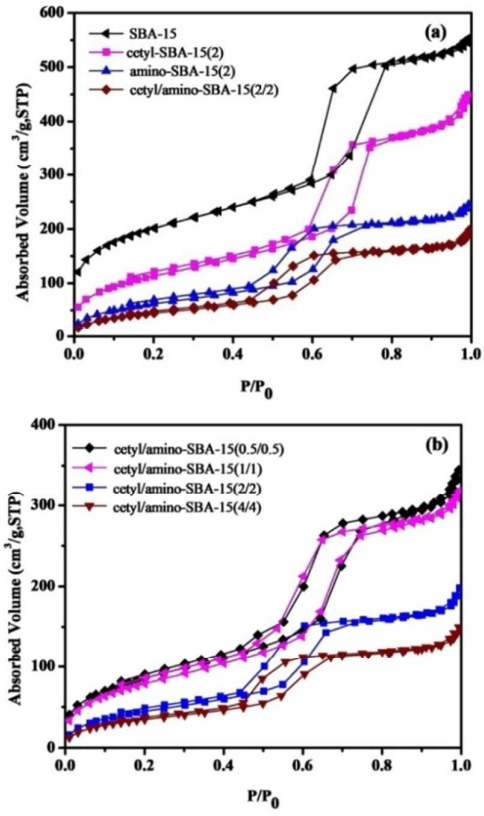

Fig. 2. N_2 adsorption/desorption isotherms of SBA-15 and functionalized SBA-15: (a) SBA-15, cetyl-SBA-15(2), amino-SBA-15(2) and cetyl/amino-SBA-15(2/2); (b) cetyl/amino-SBA-15 with different dosage.

(200) reflection planes did not change obviously, indicating that the 2D hexagonal ordered mesostructure of the prepared samples were still retained. These results suggest that the typical long-range hexagonal mesostructure still remained after introduction of organic functional groups.

The N_2 adsorption-desorption isotherms of SBA-15 and functionalized SBA-15 are shown in Fig. 2. All samples showed typical type-IV isotherms with an H1 hysteresis loop, which is characteristic of an ordered mesostructure. The porous properties of SBA-15 and functionalized SBA-15 obtained from N_2 adsorption-desorption isotherms are displayed in Table 1. The BET surface area, pore size and total pore volume of SBA-15 decreased after grafting, because partial organic functional groups loaded on the inner pore caused a pore-blocking effect. The BET surface area and pore volume decreased with the increase in the dosage of the organic modifier. The pore size of SBA-15 after grafting of functional groups decreased a little. The amount of grafted cetyl groups was relatively small, and the amino groups have a short chain and a small molecular size, thus the organic modification had little effect on the pore size. The open pore channels and high surface areas were beneficial for the rapid adsorption of the target pollutant. The BET surface area, pore size and total pore volume of cetyl-SBA-15 were much larger than that of amino-SBA-15. Though the dosage of cetyl and amino groups was the same, the steric hindrance effect of cetyl groups was much larger than that of the amino groups, although the number of grafted cetyl groups was much smaller than that of the amino groups. In comparing the cetyl/amino-SBA-15 with different mole ratios, the BET surface area, total pore volume and pore size decreased with a decrease in the mole ratio of

Table 1. Porous properties of SBA-15 and functionalized SBA-15.

Adsorbent	N_2 adsorption/desorption		
	S_{BET}(m^2/g)	V_P(cm^3/g)	D_P(nm)
SBA-15	716	0.80	5.98
cetyl-SBA-15(2)	417	0.71	5.85
amino-SBA-15(2）	236	0.39	5.73
cetyl/amino-SBA-15(0.5/0.5)	318	0.55	5.79
cetyl/amino-SBA-15(1/1)	298	0.51	5.77
cetyl/amino-SBA-15(2/2)	172	0.31	5.72
cetyl/amino-SBA-15(4/4)	133	0.23	5.56
cetyl/amino-SBA-15(1.3/2.7)	193	0.34	5.61
cetyl/amino-SBA-15(2.7/1.3)	215	0.38	5.76
cetyl/amino-SBA-15(3.2/0.8)	276	0.51	5.83
cetyl/amino-SBA-15(3.55/0.45)	323	0.61	5.87

S_{BET}: BET surface area; Vp: pore volume, P/P_0=0.97; Dp: pore diameter calculated by BJH model.

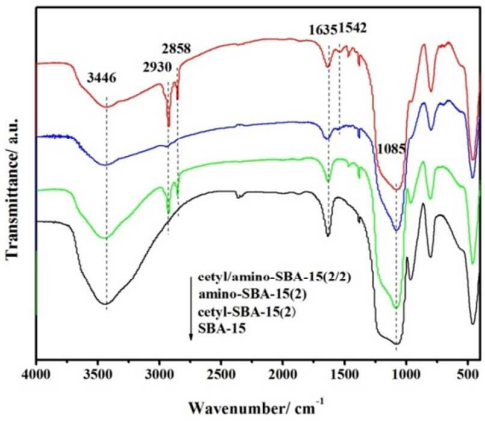

Fig. 3. FT-IR spectra of SBA-15 and functionalized SBA-15.

cetyl/amino, due to the larger steric hindrance effect of the cetyl groups.

Fig. 3 shows the FT-IR spectra of SBA-15 and functionalized SBA-15 samples. The SBA-15 exhibited three highly intense peaks. The peak at 3446 cm^{-1} could be ascribed to stretching vibration of–OH, the peak at 1635 cm^{-1} was assigned to bending vibration of H-OH, and the peak at 1085 cm^{-1} was the characteristic peak of Si-O-Si.[41,42] Compared to SBA-15, the intensity of -OH for functionalized SBA-15 was decreased, indicating that the functionalized SBA-15 was more hydrophobic than SBA-15. Cetyl-SBA-15 showed two additional highly intense peaks at 2930 and 2858 cm^{-1}, corresponding to the antisymmetric stretching vibration and symmetric stretching vibration of $-CH_2$ and $-CH_3$ on the cetyl groups.[43] Only one weak antisymmetric stretching vibration of $-CH_2$ and $-CH_3$ was observed in the FT-IR spectra of amino-SBA-15, due to the low $-CH_2$ content of the amino groups. Amino-SBA-15 showed an additional weak peak at 1542 cm^{-1}, which was ascribed to the bending vibration of –NH.[44] The characteristic peaks of the cetyl and amino groups were all observed in the FT-IR spectra of cetyl/amino-SBA-15, indicating that the cetyl and amino groups were simultaneously incorporated into SBA-15.

The CHN elemental analysis was conducted to quantitatively determine the number of the amino and cetyl groups incorporated into the surface of SBA-15. Table 2 lists the chemical properties of the functionalized SBA-15 samples. The CHN elemental analysis indicated that the amino or/and cetyl groups were successfully functionalized on the surface of the SBA-15. Comparing cetyl-SBA-15 with cetyl/amino-SBA-15, the grafted cetyl groups of cetyl-SBA-15 and cetyl/amino-SBA-15 was 0.41 mmol/g and 0.54 mmol/g, respectively. It could be inferred that appropriate amount amino groups facilitated the immobilization of the cetyl groups. The surface became more hydrophobic after loading a certain number of 3-aminopropyl groups, which was convenient for the introduction of hydrophobic cetyl groups. Table 2 shows that the grafted amount of the organic modification groups decreased in the order of cetyl/amino-SBA-15(2/2)> cetyl/diamino-SBA-15(2/2)> cetyl/triamino-SBA-15(2/2). The larger steric hindrance effects of the diamino and triamino groups resulted in lower loading amounts compared to the amino groups. With the adding amount of the cetyl and amino groups both increased from 0.5 to 2 mmol/g, the grafted cetyl groups onto SBA-15 increased from 0.35 to 0.54 mmol/g, and the grafted amino goups onto SBA-15 increased from 0.49 to 1.45 mmol/g. When the added content was increased further, the loading amount of the cetyl groups decreased, because the steric hindrance effect of amino groups were much smaller than cetyl groups, the amino groups were easier to be immobilized on the surface of SBA-15 than the cetyl goups when they coexisted in the reaction solution, so the overload of amino groups would hinder the immobilization of the cetyl groups. With the increase in the cetyl/amino mole ratio, the loading amount of the amino groups decreased from 1.79 to 0.29 mmol/g. However, the grafted amount of the cetyl groups increased from 0.29 to 0.64 mmol/g with the increase in adding amount of cetylsilane from 1.3 to 3.2 mmol/g, and then decreased to 0.52 mmol/g when the concentration of cetylsilane further increased to 3.5 mmol/g. This might be due to the following two reasons. Firstly, the strong steric hindrance effect of the cetyl groups hindered the further loading of the cetyl groups. Secondly, when the adding mole ratio of cetyl/amino increased from 3.2/0.8 to 3.55/0.45, the content of aminosilane was too low to facilitate the loading of the cetyl group, in accordance with the result from the comparison of cetyl/amino-SBA-15(2/2) and cetyl-SBA-15(2) that appropriate amount of the amino groups were beneficial for the immobilization of the cetyl groups.

Table 2. Chemical properties of functionalized SBA-15.

sample	C(wt%)	N(wt%)	cetyl(mmol/g)	amino(mmol/g)	grafted(cetyl/amino)
amino-SBA-15(2)	9.08	3.01	/	2.15	/
cetyl-SBA-15(2)	8.67	0	0.41	/	/
cetyl/amino-SBA-15(2/2)	15.52	2.03	0.54	1.45	0.37
cetyl/diamino-SBA-15(2/2)	14.92	3.65	0.37	1.30	0.28
cetyl/triamino-SBA-15(2/2)	16.62	5.19	0.33	1.23	0.26
cetyl/amino-SBA-15 (0.5/0.5)	8.64	0.69	0.35	0.49	0.71
cetyl/amino-SBA-15(1/1)	11.49	0.94	0.47	0.67	0.70
cetyl/amino-SBA-15(4/4)	14.86	3.1	0.36	2.2	0.17
cetyl/amino-SBA-15 (1.3/2.7)	11.98	2.51	0.29	1.79	0.16
cetyl/amino-SBA-15 (2.7/1.3)	14.07	1.39	0.55	0.99	0.56
cetyl/amino-SBA-15 (3.2/0.8)	14.90	0.99	0.64	0.71	0.94
cetyl/amino-SBA-15 (3.55/0.45)	10.95	0.41	0.52	0.29	1.79

3.2. The cooperative effect on the adsorption of 4-NP

Fig. 4 shows the adsorption isotherms of SBA-15, monofunctionalized SBA-15, physical mixture of monofunctionalized SBA-15 and bifunctionalized SBA-15 for 4-NP. SBA-15 exhibited a very low adsorption affinity for 4-NP due to the weak hydrogen bond interactions between Si-OH and 4-NP.[38] The adsorption capacity of functionalized SBA-15 was much higher than that of SBA-15. And the adsorption capacity was highest for cetyl/amino-SBA-15(2/2), up to 103 mg/g, much higher than the arithmetic summation of that of cetyl-SBA-15(2) (59 mg/g) and amino-SBA-15(2) (31 mg/g). The experimental result could be reasonably explained from the following two aspects. Firstly, as the result of CHN elemental analysis, the appropriate amount amino groups facilitated the immobilization of the cetyl groups, thus the bifunctionalized SBA-15 had more cetyl groups and showed higher adsorption capacity. Secondly, this could be explained by the adsorption interactions between the adsorbent and 4-NP. The interactions between the prepared samples and 4-NP are shown in Fig. 5. NP is a weak electrolyte. Hydrogen bond/electrostatic interactions existed between the amino groups on amino-SBA-15 and the phenolic hydroxyl groups of 4-NP, and presented stronger adsorption interactions than the weak hydrogen bond interactions between Si-OH on SAB-15 and 4-NP, thus the adsorption capacity of amino-SBA-15 was higher than that of SBA-15. The hydrophobic interactions between cetyl groups on cetyl-SBA-15 and nonyl group of 4-NP were much stronger than hydrogen bond/electrostatic interactions, and the adsorption capacity of cetyl-SBA-15 was far higher than that of amino-SBA-15 and SBA-15. When cetyl/amino-SBA-15 was mixed with 4-NP aqueous solution, the cetyl/amino-SBA-15 could simultaneously interact with 4-NP by the hydrophobic interactions between the cetyl groups on cetyl-SBA-15 and the nonyl groups of 4-NP, and the hydrogen bond/electrostatic interactions of the amino groups on amino-SBA-15 and the phenolic hydroxyl groups of 4-NP. Because the cooperative adsorption interactions between bifunctionalized SBA-15 and 4-NP were much stronger than the adsorption interactions between monofunctionalized SBA-15 and 4-NP, so the adsorption capacity of bifunctionalized SBA-15 was higher than the arithmetic summation of that of monofunctionalized SBA-15. Furthermore, as seen in Fig. 4, the bifunctionalized SBA-15 showed much higher adsorption capacity than the physical mixture of monofunctionalized SBA-15 (42 mg/g). The result indicated that the adsorption interactions between the physically mixed monofunctionalized SBA-15 and 4-NP were much weaker than that between the bifunctionalized SBA-15 and 4-NP. Because the cetyl and amino groups were functionalized on the surfaces of different SBA-15, the cetyl and amino groups were not close enough to cause cooperative effect.

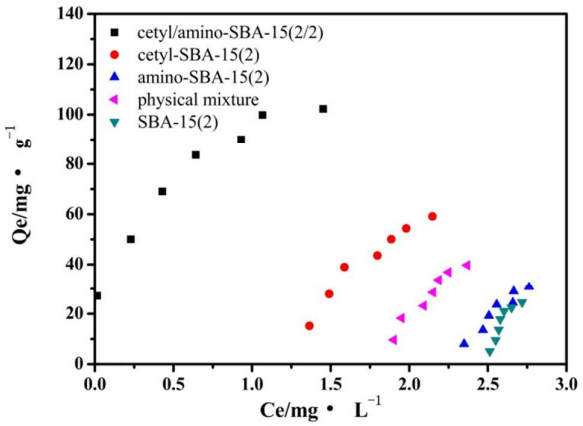

Fig. 4. Adsorption isotherms of SBA-15, monofunctionalized SBA-15, physical mixture of monofunctionalized SBA-15 and bifunctionalized SBA-15 for 4-NP.

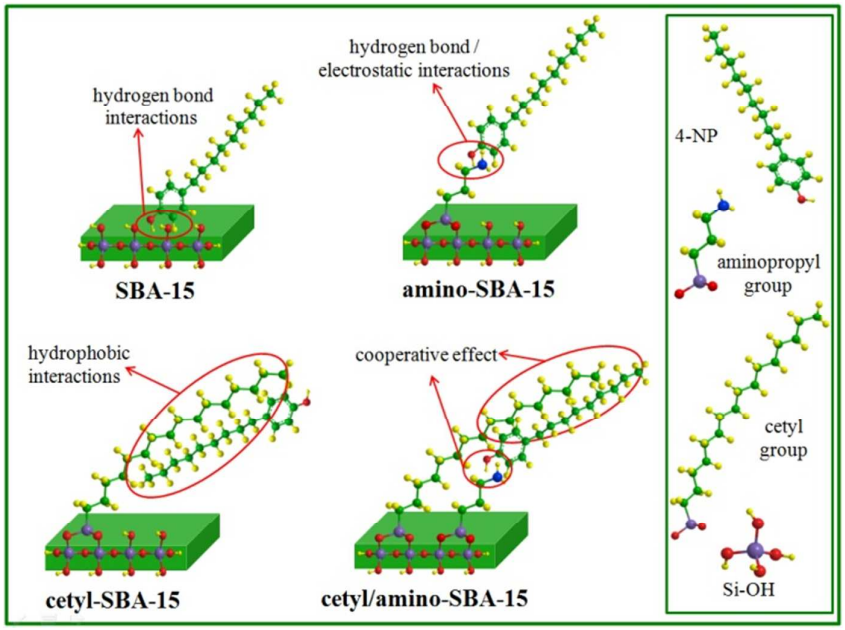

Fig. 5. Schematic illustration for the interactions between the adsorbent and 4-NP.

3.3. The effect of different amino-organoalkoxysilanes

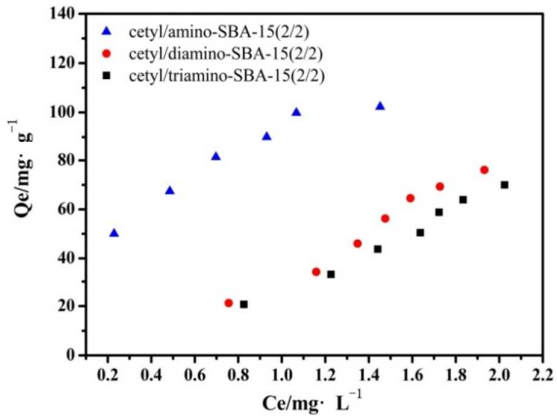

Fig. 6. Adsorption isotherms of cetyl/amino-SBA-15(2/2), cetyl/diamino-SBA-15(2/2) and cetyl/triamino-SBA-15(2/2) for 4-NP.

Amino-, diamino- and triaminosilanes were chosen to investigate the effect of -NH/-NH_2 sites on the adsorption of 4-NP. The adsorption capacities of cetyl/amino-SBA-15(2/2), cetyl/diamino-SBA-15(2/2) and cetyl/triamino-SBA-15(2/2) are shown in Fig. 6, where the adsorption capacity decreased in this order: cetyl/amino-SBA-15(2/2)> cetyl/diamino-SBA-15(2/2)> cetyl/triamino-SBA-15(2/2). The grafted mole ratio of cetyl/amino, cetyl/diamino and cety/triamino was about 0.37, 0.28 and 0.26, respectively (Table 2), the loading amount of cetyl groups were far less than amino, diamino and triamino groups. Though the -NH/-NH_2 sites in diamino and triamino groups that could form hydrogen bond/electrostatic interactions with 4-NP were more than amino groups, only one effective -NH/-NH_2 site worked with cetyl groups to cooperatively remove 4-NP, thus the effect of -NH/-NH_2 sites in amino-, diamino- and triaminosilanes on removal of NP was not obvious. In addition, the molecule size of diamino and triamino groups was bigger than that of amino groups, the larger steric hindrance effect of diamino and triamino groups resulted in a less grafted amount. As a result, cetyl/amino-SBA-15 showed the highest adsorption capacity.

3.4. The effect of dosage

The effect of cetyl- and aminosilane dosage on removal of 4-NP were investigated, as shown in Fig. 7. The adsorption capacities first increased and then decreased when the addition dose increased from 0.5 to 4 mmol/g. Cetyl/amino-SBA-15(2/2) exhibited the highest adsorption capacity, up to 103 mg/g. The experimental results were consistent with the results of the elemental analysis (Table 2). The surface densities of the amino and cetyl groups increased with the additional doses increasing from 0.5 to 2 mmol/g, and the higher loading amount of the amino and cetyl groups resulted in a higher adsorption capacity. However, the surface density of the cetyl and amino groups on cetyl/amino-SBA-15(4/4) was 0.36 mmo/g and 2.2 mmol/g with the addition concentration of the cetylsilane further increase to 4 mmol/g. The overloading of the amino groups might hinder the immobilization of the cetyl groups and resulted in a lower adsorption capacity. The BET surface area decreased with the increase of the cetyl- and aminosilane dosage from 0.5 to 2 mmol/g (Table 1). However, the adsorption capacity increased with the dosage of organic modifier, indicating that the adsorption capacity of cetyl/amino-SBA-15 for 4-NP depended on the adsorption interactions between cetyl/amino-SBA-15 and 4-NP rather than the BET surface area.

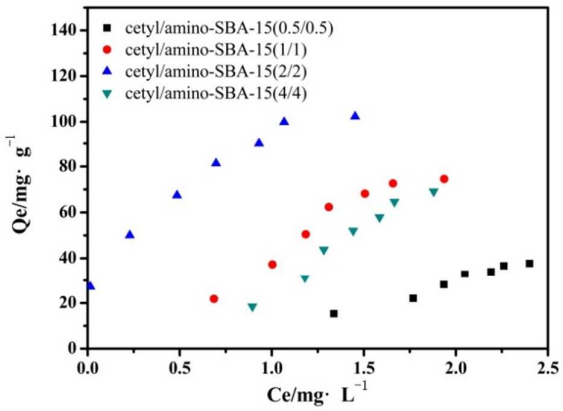

Fig. 7. Effect of dosage on the adsorption of cetyl/amino-SBA-15 for 4-NP.

3.5. The effect of different cetyl/amino mole ratios

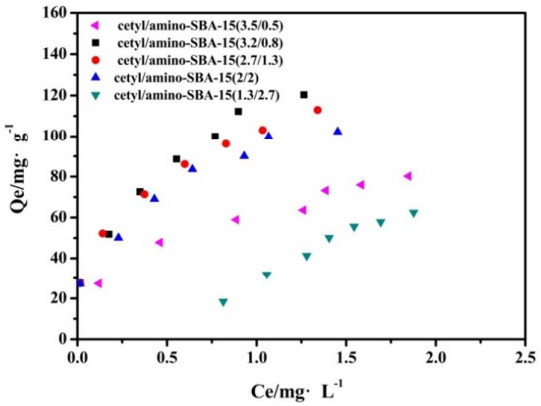

Fig. 8. Effect of different mole ratios of cetyl/amino on adsorption of cetyl/amino-SBA-15 for 4-NP.

To further reveal the cooperative effect of cetyl and aminopropyl groups, we investigated the effect of different cetyl/amino mole ratios on the adsorption isotherms of cetyl/amino-SBA-15 for 4-NP by keeping the dosage of the organic functional groups as a constant (4 mmol/g) but changing the cetyl/amino mole ratio. Fig. 8 shows that the adsorption capacity increased when the cetyl/amino mole ratio increased from 1.3/2.7 to 3.2/0.8 and then decreased with the further increase in the cetyl/amino mole ratio to 3.55/0.45. Combined Table 2 further illustrates the cooperative adsorption mechanism. The grafted mole ratio of cetyl/amino groups increased when the addition mole ratio of cetyl/amino increased from 1.3/2.7 to 3.55/0.45 (Table 2). For cetyl/amino-SBA-15(3.2/0.8), the grafted amount of cetyl and amino groups was 0.64 and 0.71 mmol/g, respectively, and the grafted mole ratio of cetyl/amino was almost equal to 1 (0.94), showing the highest

adsorption capacity, up to 120 mg/g (Fig. 8). As seen in Fig. 5, it would cause cooperative effect when one cetyl group and one amino group simultaneously bind with 4-NP, the amount of cetyl and amino groups cooperatively participated in the removal of 4-NP achieved maximum when the grafted mole ratio of cetyl/amino was 1:1, so the highest adsorption capacity was obtained. For cetyl/amino-SBA-15(3.55/0.45), the surface density of cetyl groups was 0.52 mmol/g close to cetyl/amino-SBA-15(2.7/1.3) (0.55 mmol/g) and cetyl/amino-SBA-15(2/2) (0.54 mmol/g), the grafted amino groups was 0.29 mmol/g far less than that of cetyl/amino-SBA-15(2.7/1.3) (0.99 mmol/g) and cetyl/amino-SBA-15(2/2) (1.45 mmol/g), and the adsorption capacity was much less than that of cetyl/amino-SBA-15(2.7/1.3) and cetyl/amino-SBA-15(2/2), thus the loading amount of the amino groups was the major limiting factor for 4-NP adsorption. These results further indicated that the cooperative effect between cetyl and amino groups was the predominant factor in remarkably improving the adsorption capacity. Interestingly, the loading amount of cetyl groups on cetyl/amino-SBA-15(3.55/0.45) (0.29 mmol/g) was equal to the grafted amount of the amino groups on cetyl/amino-SBA-15(1.3/2.7) (0.29 mmol/g), while the former showed higher adsorption capacity than the latter. This suggested that besides the cooperative interactions of the cetyl and amino groups, the interaction between the residual cetyl groups on cetyl/amino-SBA-15(3.55/0.45) and 4-NP was stronger than that between the residual amino groups on cetyl/amino-SBA-15(1.3/2.7), in accordance with the result that the adsorption capacity of monofunctionalized cetyl-SBA-15 was much higher than that of amino-SBA-15 (Fig. 4). Therefore, further adsorption performance researches were performed using cetyl/amino-SBA-15(3.2/0.8) as a representative adsorbent.

3.6. The effect of pH

The solution pH is an important factor affecting the adsorption process, which not only can change the surface charge of the adsorbent but also can influence the degree of ionization of the target pollutant. To reveal the effect of pH on the adsorption of 4-NP by cetyl/amino-SBA-15, the pH of the initial solutions was adjusted by NaOH (0.1 M) and HCl (0.1 M) from 4 to 12. The experimental results are illustrated in Fig. 9. When the pH increased from 4 to 9, the adsorption capacity of cetyl-amino-SBA-15 changed very slightly, indicating that the cetyl-amino-SBA-15 showed high adsorption capacity over a wide pH range. When the pH>9, the adsorption capacity decreased remarkably due to the electrostatic

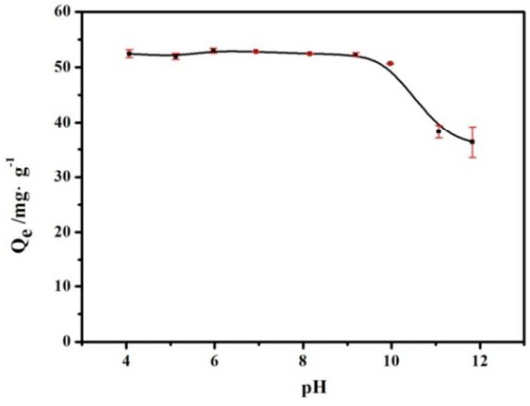

Fig. 9. Effect of pH on the adsorption of cetyl/amino-SBA-15 for 4-NP.

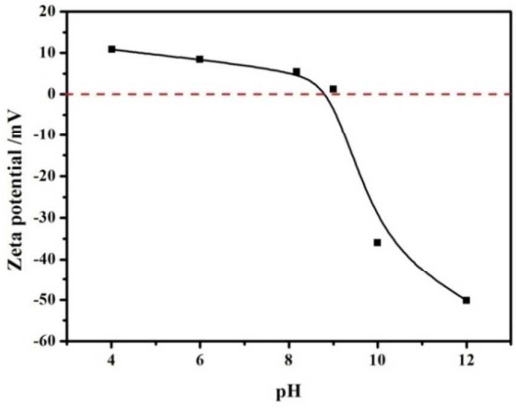

Fig. 10. Zeta potentials of cetyl/amino-SBA-15.

repulsion between 4-NP and the adsorbents. To further investigate the surface charge of cetyl/amino-SBA-15, zeta potentials were determined. The zeta potentials of cetyl/amino-SBA-15 at different pH values are displayed in Fig. 10. When the pH was in the range of 4~9, the zeta potentials of cetyl- amino-SBA-15 were all positively charged and decreased slightly with the increase in pH. Under these conditions, the grafted amino group could form protonated -NH_3^+. Hydrogen bond/electrostatic interactions between 4-NP and the amino groups and hydrophobic interactions between 4-NP and the cetyl groups were the predominant interactions. Fig. 10 shows that the isoelectric point of cetyl-amino-SBA-15 was approximately at pH=9. When the pH>9, the zeta potentials decreased remarkably. As the pH increased, the number of hydroxyl groups adsorbed on the bifunctionalized SBA-15 increased, and the surface negative charge of the cetyl/amino-SBA-15 increased. Moreover, the protonated -NH_3^+ reverted to the free amine form, leading to the rapid decline of the surface charge. The dissociation constant (pKa) of 4-NP is reported to be 10.7±1.0.[45,46] When the pH>pKa, 4-NP would be deprotonated and form 4-NP^-. The electrostatic repulsion between 4-NP and the adsorbents was the predominant interaction and resulted in a low adsorption capacity.

3.7. The selectivity of cetyl/amino-SBA-15

The high concentrations of organic pollutants with low toxicity existing in wastewater will primarily occupy the adsorption sites and hinder the adsorption of low concentration organic pollutants with high toxicity. Ph exists widely in wastewater at a high concentration, and the molecular structure is similar to 4-NP (Table 3). Ph was chosen as a competitive pollutant to investigate the selectivity of cetyl/amino-SBA-15 for 4-NP. The adsorption capacity of cetyl/amino-SBA-15 with different $C_{4\text{-NP}}$:C_{Ph} ratios is displayed in Fig. 11. The cetyl/amino-SBA-15 showed high selectivity for 4-NP against Ph. The adsorption capacity of Ph increased with the increase in Ph concentration, but the adsorption capacity of 4-NP almost keeping a constant, illustrated the Ph concentration have little influence on the adsorption of 4-NP. The selective adsorption coefficients were used to compare the selectivity of prepared samples at different $C_{4\text{-NP}}$:C_{Ph} ratios, as seen in Table 4. The selective

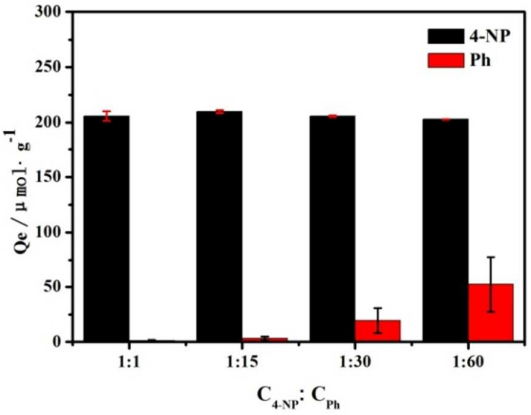

Fig. 11. Adsorption capacity of cetyl/amino-SBA-15 with different C_{NP}:C_{Ph}.

Table 3. Property parameters of 4-NP and Ph.

chemicals	structure	M	S_w (25 °C, mg/L)	logK_{ow}
4-nonylphenol	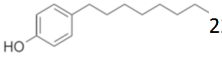	220.24	5.43	4.48
phenol		94.11	8000	1.50

adsorption coefficients of 4-NP at different values of $C_{4\text{-}NP}$:C_{Ph} were higher than 1400, reaching up to 2055 when $C_{4\text{-}NP}$:C_{Ph} was 1:30, indicating that the cetyl/amino-SBA-15 showed a high selectivity for 4-NP. The logK_{ow} of 4-NP (4.48) was much higher than the logK_{ow} of Ph (1.50)(Table 3), due to the hydrophobic nonyl groups in 4-NP. When cetyl/amino-SBA-15 mixed with the Ph and 4-NP mixture solutions, Ph could interact with the amino groups of cetyl/amino-SBA-15 by hydrogen bond/electrostatic interactions and bind residual Si-OH by hydrogen bond interactions. In addition to the hydrogen bond/electrostatic interactions, the nonyl groups of 4-NP could strongly bind the cetyl groups on cetyl/amine-SBA-15 through hydrophobic interactions. The adsorption interactions between 4-NP and cetyl/amine-SBA-15 were much stronger than that between Ph and cetyl/amine-SBA-15, thus 4-NP would be primarily adsorbed on the cetyl/amine-SBA-15.

Table 4. Selective adsorption coefficients of NP in mixed solution with different C_{NP}: C_{Ph}.

C_{NP}: C_{Ph}	1:1	1:15	1:30	1:60
K_{NP}	5.771	5.806	4.891	4.622
K_{Ph}	0.00408	0.00296	0.00238	0.00309
$K_{NP,\ Ph}$	1414	1961	2055	1496

3.8. Regeneration performance of the adsorbent

The regeneration performance of the adsorbent is an important factor for the wide applications, making it beneficial to reduce the cost of the adsorbent. NaOH solution (0.1 M) was used to regenerate the saturated adsorbent. The regenerated adsorbent was reused in the next run under the same conditions. The regenerated and recycled results of cetyl/amino-SBA-15 are shown in Fig. 12. Cetyl/amino-SBA-15 had a stable and excellent adsorption capacity for 4-NP after five cycles. The adsorption capacity of cetyl/amino-SBA-15 decreased slightly after three cycles, probably attributed to a partial loss of the organic functional groups from cetyl/amino-SBA-15 during the regeneration process. As a result, cetyl/amino-SBA-15 could be recycled several times retaining a stable and excellent adsorption capacity.

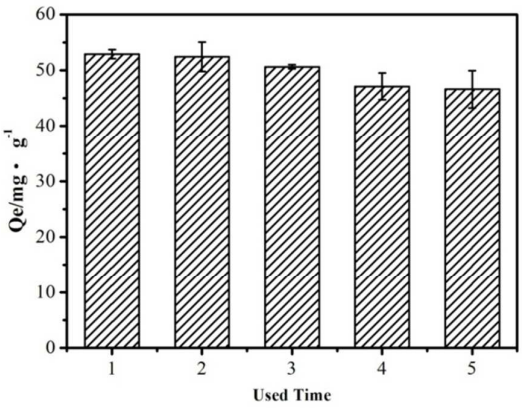

Fig. 12. Recovery and regeneration performance of cetyl/amino-SBA-15 for removal of 4-NP.

4. Conclusions

In this work, cetyl/amino-SBA-15 was successfully synthesized by a post-synthesis grafting method. The adsorption capacity of bifunctionalized SBA-15 was remarkably higher than that of monofunctionalized and unmodified SBA-15, attributed to the cooperative effect of hydrogen bond/electrostatic interactions between 4-NP and the amino groups and hydrophobic interactions between 4-NP and the cetyl groups. The cetyl/amino-SBA-15 showed a high adsorption capacity for 4-NP over a wide range of pH values. The distribution of cetyl and amino groups played a key role in the adsorption capacity of cetyl/amino-SBA-15. Cetyl/amino-SBA-15(3.2/0.8) showed the highest adsorption capacity, up to 120 mg/g. The high selectivity for 4-NP and the excellent adsorption capacity after recycling several times caused cetyl/amino-SBA-15 to have great potential for wastewater treatment.

Acknowledgments

This work was supported by the Natural Science Foundation of China (No. 21277051, 21037001) and the Science and Technology Planning Project of Guangzhou City (No. 12C62081602).

References:

1 J. Huang, X. Zhang, S. Liu, Q. Lin, X. He, X. Xing, W. Lian and D. Tang, *Sensor. Actuat. B: Chem.*, 2011, **152**, 292-298.

2 P. Gao, Z. Li, M. Gibson and H. Gao, *Chemosphere*, 2014, **104**, 113-119.

3 Y. Niu, J. Zhang, H. Duan, Y. Wu and B. Shao, Y. Wu and B. Shao, *Food Chem.*, 2015, **167**, 320-325.

4 G. Correa-Reyes, M. T. Viana, F. J. Marquez-Rocha, A. F. Licea, E. Ponce and R. Vazquez-Duhalt, *Chemosphere*, 2007, **68**, 662-670.

5 R. A. Rudel, D. E. Camann, J. D. Spengler, L. R. Korn and J. G. Brody, *Environ. Sci. Technol.*, 2003, **37**, 4543-4553.

6 G. Ying, B. Williams and R. Kookana, *Environ. Int.*, 2002, **28**, 215-226.

7 B. Shao, J. Hu, M. Yang, W. An and S. Tao, *Arch. Environ. Con. Tox.*, 2005, **48**, 467-473.

8 J. Shan, Y. Wang, L. Wang, X. Yan and R. Ji, *Environ. Pollut.*, 2014, **189**, 202-207.

9 T. Isobe, H. Nishiyama, A. Nakashima and H. Takada, *Environ. Sci. Technol.*, 2001, **35**,1041-1049.

10 M. Staniszewska, L. Falkowska, P. Grabowski, J. Kwaśniak and S. Mudrak-Cegiołka, A. R. Reindl, A. Sokołowski, E. Szumiło and A. Zgrundo, *Arch. Environ. Con. Tox.*, 2014, **67**, 335-347.

11 S. Ömeroğlu and F.D. Sanin, *Water Res.*, 2014, **64**, 1-12.

12 J.P.A. De Weert, M. Viñas, T. Grotenhuis, H.H.M. Rijnaarts and A.A.M. Langenhoff, *Biodegradation*, 2011, **22**, 175-187.

13 B.V. Chang, F. Chiang and S.Y. Yuan, *Chemosphere*, 2005, **60**, 1652-1659.

14 K. Inumaru, M. Murashima, T. Kasahara and S. Yamanaka, *Appl. Catal. B: Environ.*, 2004, **52**, 275-280.

15 S. Naya, T. Nikawa, K. Kimura and H. Tada, *ACS Catal.*, 2013, **3**, 903-907.

16 Z. Lu, J. Gan, *Environ. Pollut.*, 2013, **180**, 214-220.

17 M. Barhoumi, I. Beurroies, R. Denoyel, H. Saïd and K. Hanna, *Colloid Surface A*, 2003, **219**, 25-33.

18 K.J. Choi, S.G. Kim, C.W. Kim and S.H. Kim, *Chemosphere*, 2005, **58**, 1535-1545.

19 Z. Yu, S. Peldszus and P.M. Huck, *Water Res.*, 2008, **42**, 2873-2882.

20 B. Pan, D. Lin, H. Mashayekhi and B. Xing, *Environ. Sci. Technol.*, 2008, **42**, 5480-5485.

21 T. Yokoi, H. Yoshitake and T. Tatsumi, *J. Mater. Chem.*, 2004, **14**, 951-957.

22. K. Ariga, A. Vinu, Y. Yamauchi, Q. Ji, and J. P. Hill, *B. Chem. Soc. Jpn.*, 2012, **85**, 1-32.

23.Y. Yang, C. Liu, Y. Liang, F. Lin, and K. C. W. Wu, *J. Mater. Chem. B,* 2013, **1**, 2447-2450.

24. B. P.Bastakoti, S. Ishihara, S. Leo, K. Ariga, K. C. W. Wu, and Y. Yamauchi, *Langmuir,* 2014, **30**, 651-659.

25. T. Nguyen-Phan, C. Y. Lee, J. S. Chung and E. W. Shin, *Res. Chem. Intermediat.*, 2008, **34**, 743-753.

26. H. Li, J. Wang, H. Li, S. Yin and T. Sato, *Res. Chem. Intermediat.*, 2010, **36**, 27-37.

27. Y. Yamachi, *J. Ceram. Soc. Jpn.*, 2013, **121**, 831-840.

28. K. Ariga, Y. Yamauchi, G. Rydzek, Q. Ji, Y. Yonamine, K. C. W. Wu, and J. P. Hill, *Chem. Lett.,* 2014, **43**, 36-68.

29. F.Shieh, S.Wang, S. Leo and K. C. W. Wu, *Chem-Eur. J.*, 2013, **19**, 11139-11142.

30 K. Inumaru, J. Kiyoto and S. Yamanaka, *Chem. Commun.*, 2000, **11**, 903-904.

31 Y. Kim, B. Lee, K. Choo and S. Choi, *Micropor. Mesopor. Mat.*, 2014, **185**, 121-129.

32 C. Ling, F. Liu, C. Xu, T. Chen and A. Li, *ACS Appl. Mater. Inter.*, 2013, **5**,11808-11817.

33 J. Shi, 2013, **113**, 2139-2181.

34 Y. Ide and M. Ogawa, *Angew Chem. Int. Edit.*, 2007, **46**, 8449-8451.

35 Y. Ide, S. Iwasaki and M. Ogawa, *Langmuir*, 2011, **27**, 2522-2527.

36 Y. Zhang, Z. Qiao, Y. Li, Y. Liu and Q. Huo, *J. Mater. Chem.*, 2011, **21**, 17283-17289.

37 D. Zhao, J. Feng, Q. Huo, N. Melosh, G.H. Fredrickson, B.F. Chmelka and G.D. Stucky, *Science*, 1998, **279**, 548-552.

38 Y. Kim, B. Lee, K. Choo and S. Choi, *Micropor. Mesopor. Mat.*, 2011, **138**, 184-190.

39 Z. Guo, S. Zheng, Z. Zheng, F. Jiang and W. Hu, L. Ni, *Water Res.*, 2005, **39**, 1174-1182.

40 X.F. Qian, T. Kamegawa, K. Mori, H.X. Li and H. Yamashita, *J. Phys. Chemi. C*, 2013, **117**, 19544-19551

41 Y. Hu, Y. He, X. Wang and C. Wei, *Appl. Surf. Sci.*, 2014, **311**, 825-830.

42 Z. Li, K. Su, B. Cheng and Y. Deng, *J. Colloid .Interf. Sci.*, 2010, **342**, 607-613.

43 H. Niu and Y. Cai, *Anal. Chem.*, 2009, **81**, 9913-9920.

44 G.B.B. Varadwaj, S. Rana and K.M. Parida, *Dalton T.*, 2013, **42**, 5122-5129.

45 N.H. Ince, I. Gültekin and G. Tezcanli-Güyer, *J. Hazard. Mater.*, 2009, **172**, 739-743.

46 R. Vazquez Duhal, Nonylphenol, *Appl. Ecol. Env. Res.*, 2006, **4**, 1-25.